



CHORUS

This is the accepted manuscript made available via CHORUS. The article has been published as:

Anisotropic Ion Heating and Tail Generation during Tearing Mode Magnetic Reconnection in a High-Temperature Plasma

R. M. Magee, D. J. Den Hartog, S. T. A. Kumar, A. F. Almagri, B. E. Chapman, G. Fiksel, V. V. Mirnov, E. D. Mezonlin, and J. B. Titus

Phys. Rev. Lett. **107**, 065005 — Published 4 August 2011

DOI: [10.1103/PhysRevLett.107.065005](https://doi.org/10.1103/PhysRevLett.107.065005)

Anisotropic ion heating and tail generation during tearing mode magnetic reconnection in a high-temperature plasma

R. M. Magee,^{1,*} D. J. Den Hartog,^{1,2} S. T. A. Kumar,^{1,2} A. F. Almagri,^{1,2}
B. E. Chapman,¹ G. Fiksel,^{1,2,†} V. V. Mirnov,^{1,2} E. D. Mezonlin,³ and J. B. Titus³

¹*Department of Physics, University of Wisconsin - Madison, Madison, WI 53706, USA*

²*Center for Magnetic Self-Organization in Laboratory and Astrophysical Plasmas, Madison, WI 53706, USA*

³*Department of Physics, Florida A & M University, Tallahassee, FL 32307, USA*

Complementary measurements of ion energy distributions in a magnetically-confined high-temperature plasma show that magnetic reconnection results in both anisotropic ion heating and the generation of suprathermal ions. The anisotropy, observed in the C^{+6} impurity ions, is such that the temperature perpendicular to the magnetic field is larger than the temperature parallel to the magnetic field. The suprathermal tail appears in the majority ion distribution and is well-described by a power-law to energies 10 times the thermal energy. These observations may offer insight into the energization process.

A hallmark of magnetic reconnection is the conversion of magnetic energy into particle kinetic energy. This process manifests itself in a variety of ways, two of which are ion heating and ion tail generation. Ion heating at rates much faster than the electron-ion energy transfer time is observed in reversed field pinches (RFP) [1–4] and laboratory reconnection experiments [5], and at locations far from obvious heating sources in the solar corona [6, 7]. In the Madison Symmetric Torus (MST) RFP [8], magnetic reconnection due to resonant tearing instabilities liberates a large amount of energy from the magnetic field in a short amount of time, a significant fraction of which (10 – 25%) appears as ion thermal energy [9]. Models of ion heating based on ion cyclotron damping of Alfvénic fluctuations [10, 11], viscous damping of tearing mode flows [12, 13], and stochastic heating [9] have all been applied with varying degrees of success, but no single theory is able to explain all of the observed features of the heating. Non-thermal energization from reconnection has also been observed in a variety of plasma systems. In the laboratory, small populations of suprathermal ions have been explained with parallel electric field acceleration [14–16]. In the Earth’s magnetosphere, electrons with energies 10^5 times larger than the energy in the large-scale flow form a power-law tail in the energy spectrum, consistent with a particle-in-cell model of Fermi acceleration [17]. Previous measurements on MST have shown the beginning of a tail in the ion distribution [18], but it has never been fully resolved.

In this Letter we present experimental measurements of ion energy distributions in MST plasmas which reveal new details about both forms of energization, offering insight into the underlying physics. First, charge exchange recombination spectroscopy (CHERS) measurements of the C^{+6} impurity ion temperature in the core parallel (T_{\parallel}) and perpendicular (T_{\perp}) to the mean magnetic field reveal a local anisotropy in which $T_{\perp} > T_{\parallel}$ near in time to the reconnection. This observation indicates that the thermal heating mechanism favors the perpendicular degree of freedom, a constraint in discriminating among the aforementioned theoretical models. Second, measurements of the D-D fusion neutron flux and of neutral energy spectra indicate a population of suprathermal ions

is generated during magnetic reconnection. These fast ions represent a few percent of the total ion population, and the spectrum is well-described by a power-law. It is not yet clear whether the ion heating and the generation of the tail are the results of the same physical process or of distinct mechanisms.

A typical MST discharge is punctuated by discrete bursts of magnetic reconnection. The plasma is formed and the bulk of the confining magnetic field is generated by inductively driving current around the toroid, a process which naturally leads to a current density gradient. This gradient is a free energy source for tearing mode instabilities, which redistribute current to flatten the gradient and allow the plasma to relax to a lower energy state [19]. The mechanism responsible for the plasma relaxation is tearing mode reconnection which occurs at resonant surfaces in the plasma where the perturbation wave vector is perpendicular to the magnetic field. There, the finite plasma resistivity allows the perturbation to reconnect field lines with oppositely directed components. There are several such resonant sites in the plasma, and a spectrum of modes are spontaneously excited in the core. Subsequent mode coupling leads to a cascade of energy across spatial scales [20]. Figure 1 shows the time histories from a typical discharge of the magnetic fluctuations and the equilibrium magnetic field energy. The amplitudes of the tearing modes in the core of the plasma increase five-fold or more at each event, to relative sizes as large as 1% of the mean field. The energy stored in the equilibrium field, obtained from equilibrium reconstruction, drops by 10 kJ in $\lesssim 100 \mu\text{s}$. This is the energy source for both the heating and the acceleration. Previous measurements have shown that in deuterium plasmas the impurity C^{+6} ions are heated to a higher temperature than the bulk [21], however, due to the lower density of carbon ($n_C \sim 0.5\% n_D$) the majority of the thermal energy is carried by the bulk.

Localized measurements of the C^{+6} impurity ion temperature are made by stimulating charge exchange emission of intrinsic carbon impurities with hydrogen neutrals injected as a 50 keV diagnostic neutral beam [22]. The Doppler-broadening of this emission is measured from orthogonal viewing chords to allow a comparison of T_{\perp} and T_{\parallel} in the core of MST during the reconnection heating event. A simul-

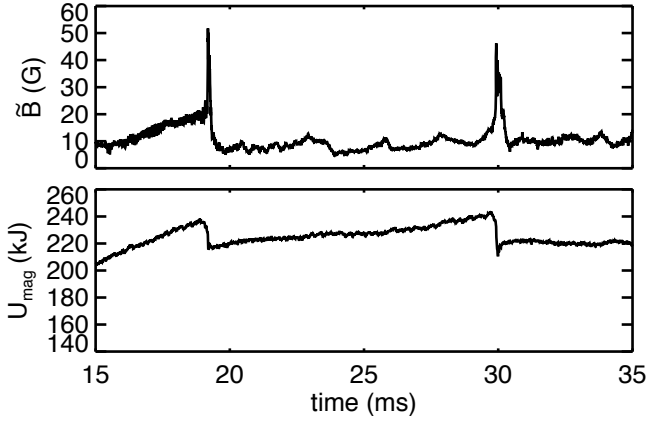


FIG. 1. Signatures of tearing mode reconnection in a typical MST discharge. The amplitude of the core mode magnetic fluctuations increases (top) and the magnetic energy decreases (bottom).

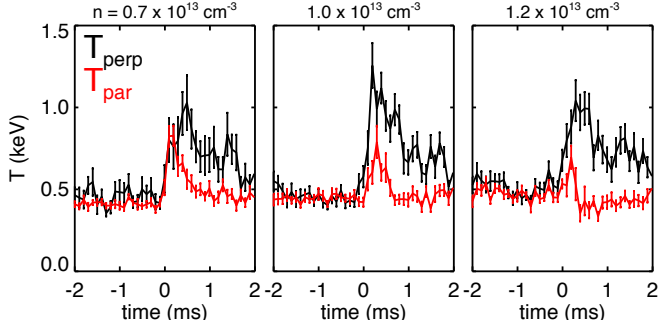


FIG. 2. The event-averaged local C^{+6} T_{\perp} (black) and T_{\parallel} (red) as functions of time, where $t = 0$ is the reconnection heating event. Three density ensembles are plotted, with density increasing left to right. The error bars represent event-to-event variation.

taneous background measurement allows radial spatial resolution of 1-2 cm and temporal resolution of 100 μ s [23, 24]. The temperatures as a function of time from many similar events are averaged together, aligned such that $t = 0$ is the maximum rate of change of magnetic flux during reconnection, and grouped into 3 density ranges. The result of this procedure is shown in Figure 2.

There are two features of the data that appear independent of changes to plasma density and one that does not. First, far in time (> 2 ms) from the reconnection event, $T_{\perp} = T_{\parallel}$. Second, the change in the perpendicular temperature, ΔT_{\perp} , defined as the maximum temperature minus the equilibrium temperature, is always larger than ΔT_{\parallel} . This implies that the reconnection heating mechanism favors the perpendicular degree of freedom. It can also be seen that as the plasma density is increased, ΔT_{\parallel} decreases while ΔT_{\perp} remains unchanged, so that the anisotropy *increases* with increasing plasma density. This observation is contrary to intuition of collisional isotropization, and contrary to the density dependence of anisotropies seen elsewhere [25].

We have adapted the equations of Cranmer et. al. [7] as in Tangri et al. [11] to test a simple model in which (1) the heating acts purely on the perpendicular degree of freedom during the short burst of magnetic reconnection and (2) the temperatures evolve due only to collisional isotropization and equilibration and finite energy confinement time. The carbon temperature is evolved according to,

$$\frac{dT_{\perp,C}}{dt} = \frac{1}{kn_C} (C_{\perp,CD} (T_{\perp,D} - T_{\perp,C}) + \sum_i m_i J_{\perp,Ci}) - \frac{T_{\perp,C}}{\tau} + Q_{\perp} \quad (1)$$

$$\frac{dT_{\parallel,C}}{dt} = \frac{2}{kn_C} (C_{\parallel,CD} (T_{\parallel,D} - T_{\parallel,C}) + \sum_i m_i J_{\parallel,Ci}) - \frac{T_{\parallel,C}}{\tau}, \quad (2)$$

where the C operators represent collisional equilibration between the majority deuterium and carbon, and the J operators represent the collisional isotropization of the carbon on all known MST impurities: B, C, N, O, Al (see Ref. [7] for definitions of the C and J operators). The effect of the bulk ion heating is included by using the $T_{D,\perp}$ as measured by the Rutherford scattering diagnostic [26], and we assume $T_{D,\parallel} = T_{D,\perp}$ (measurements of $T_{D,\parallel}$ are not currently available). We also assume that all impurities have the same temperature. Q_{\perp} is an ad hoc heating term active from $-0.05 < t < +0.1$ ms. We use $Q_{\perp} = 10$ MeV/s to reproduce the observed temperature increase. Finally, the finite energy confinement is modeled with the last term, with $\tau = 1$ ms.

It is found that this model reproduces some but not all of the features of the data. It is seen in Figure 3 that $\Delta T_{C,\perp} > \Delta T_{C,\parallel}$, which we interpret as evidence that the heating mechanism does in fact favor the perpendicular degree of freedom. Furthermore, we have uncovered a relatively simple explanation for the inverse density dependence of ΔT_{\parallel} - varying impurity concentration in the plasma. The heavy carbon ions are scattered more efficiently by other impurities than by deuterium, so the isotropization rate is sensitive to the impurity content. Measurements of x-ray bremsstrahlung radiation indicate that the effective ionic charge of the plasma, $Z_{eff} = \sum_i n_i Z_i^2 / n_e$ (the sum is over all ion species), decreases with increasing plasma density. This is due to both reduced dilution and lower electron temperature (the latter affects the impurity charge state distribution). It can be seen in Figure 3 that a decrease in Z_{eff} from 4.3 in the low density case to 2.5 in the high density case results in lower ΔT_{\parallel} in the high density case, consistent with the data. There are some differences however. In particular, the temperature decay time is shorter in the model. This is because the collision frequency of the carbon impurities is large (~ 10 kHz) due to their high charge. The implication of the data then is that the heating process is active for more than just the time of the impulsive burst of reconnection. This is not inconsistent with the magnetic field measurements. The magnetic fluctuations are in fact always present at a low level (see Figure 1), so it may

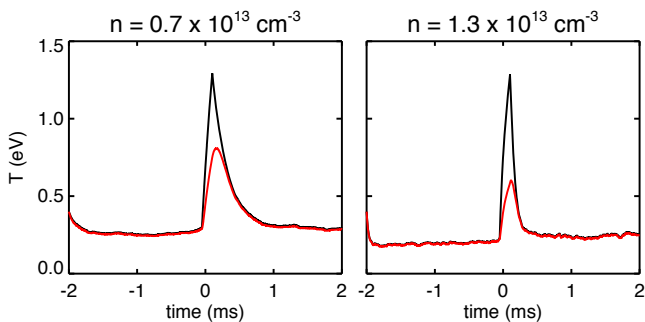


FIG. 3. Evolution of $T_{C,\perp}$ (black) and $T_{C,\parallel}$ (red) according to the collisional model described in the text with impulsive, perpendicular heating. The temperature decays more quickly than in the data (see Figure 2), but the observed behavior of the anisotropy is reproduced by varying Z_{eff} from 4.3 in the low density case to 2.5 in the high density case.

be the case that there is both an impulsive burst of heating and a continuous, low level simmer.

A neutral particle analyzer (NPA) can be used to measure the ion energy distribution and complements the Doppler-based measurements (which are sensitive to thermal broadening) in its ability to resolve small numbers of high energy particles. Previous work has shown that, in some cases, the beginning of a high energy tail in the distribution function is observed [18]. Here we present new data from an NPA with a larger energy range ($0.34 < E < 5.2$ keV) and improved energy resolution which allow a more complete characterization of this feature.

A plasma ion can undergo charge exchange with a neutral atom and, if it avoids re-ionization, escape to the edge. The flux of neutral atoms is proportional to the product of the probabilities that these events occur. We measure the energy of these charge exchange neutrals with a radially-viewing 25 channel analyzer [27]. Using information known about the neutral density profile and the plasma parameters which determine the attenuation (n_e, T_e, n_i), information about the ion energy distribution function can be extracted from the neutral spectrum.

The measured neutral particle flux departs significantly from that expected from a thermal ion distribution for energies $E > 1200$ eV (see Figure 4). We find that the functional form of this distribution is well-described by a Maxwellian with a small power-law perturbation (i.e. $f_i(E, \vec{x}) = f_{i0}(E, \vec{x}) + n_{fi}(\vec{x})E^{-\gamma}$, where f_{i0} is a standard Maxwellian, n_{fi} is the fast ion density, E is the energy and γ is the spectral index). The total number of suprathermal ions is just a few percent of the total ion population, but the total energy content of the population can be an appreciable fraction of the internal energy of the thermal component. The spectral index is plotted as a function of time in Figure 5. It decays after energization at a rate roughly consistent with classical slowing down, indicating that the tail is generated during the reconnection.

The existence of the suprathermal deuterium population is

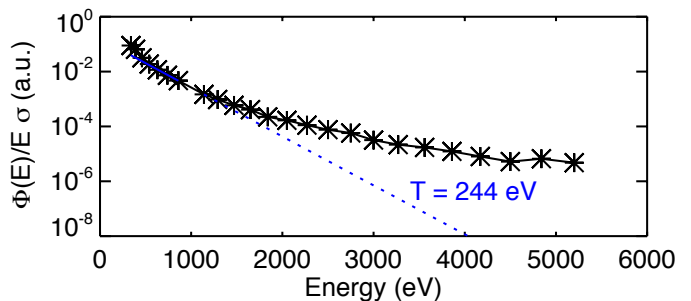


FIG. 4. Neutral particle flux measured shortly after a reconnection event clearly showing a high energy tail. The expectation for a thermal distribution is shown with the dashed line. (Note that the inferred temperature is lower than that measured with CHERS due to line-of-sight integration of the temperature profile and the lower bulk ion temperature.)

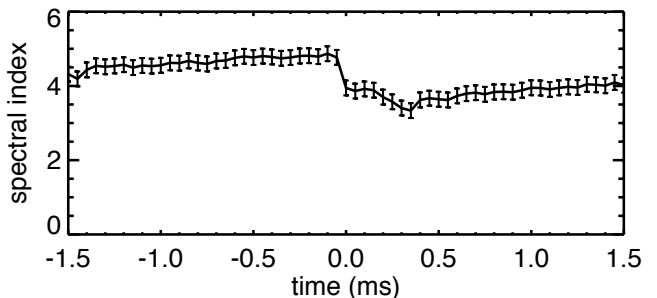


FIG. 5. The spectral index of the power-law tail of the ion distribution as a function of time. The decay in the tail after the reconnection is consistent with classical slowing down. The error bars are the uncertainty in the fitting.

corroborated by scintillator measurements of D-D fusion neutrons. The D-D fusion cross section is extremely sensitive to ion energy, so a small number of fast ions can contribute more to the total neutron flux than the entire thermal population, and, in fact, the measured neutron flux from MST discharges exceeds that expected from thermal fusion alone. Plotted in Figure 6 is the event-averaged measured neutron emission (blue) compared to two calculated emission rates: one based on thermal fusion (red) and one based on the ion distribution function inferred from the NPA measurements and extrapolated to 20 keV (black). From the large disagreement between the measured neutron rate and the rate calculated using the Maxwellian assumption, we conclude that the neutron production from MST plasmas is completely dominated by the fast ions. Furthermore, the agreement between the measured rate and the rate calculated from the extrapolated spectrum indicates that the fast ion population is even larger than what is measured by the NPA.

One possible mechanism for producing fast ions is electric field acceleration [15]. In MST, a large, parallel electric field is induced at the reconnection event. It is ~ 50 V/m

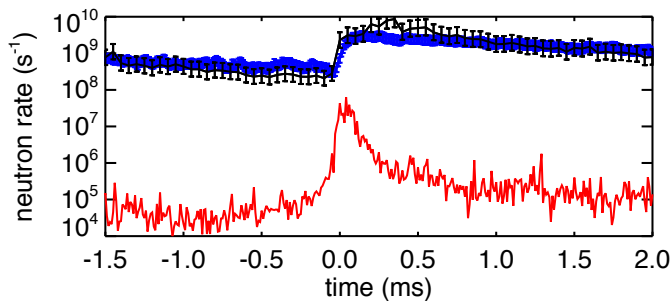


FIG. 6. A comparison of the measured neutron emission (blue) to a calculation of emission due to thermal fusion based on the measured temperature (red) and a calculation based on the ion distribution inferred from NPA measurements and extrapolated to 20 keV (black). The agreement between the blue and black curves implies that neutron production is fast ion-dominated in MST.

in magnitude and lasts for $\sim 100 \mu\text{s}$. Although electric field acceleration of ions is balanced by frictional drag on drifting electrons in a simple electron-ion plasma, this balance is upset when impurities are introduced. The frictional drag on a test ion with charge Z due to drifting electrons can be combined with the electric field to form the effective electric field, $E^* = E(1 - Z/Z_{eff})$ [14], from which it can be seen that, for typical MST values of $Z_{eff} \sim 4$, a deuteron can experience up to 3/4 of the applied field. Although a thermal ion will only be accelerated to ~ 1 keV, faster ions can reach higher energies. Furthermore, it has been observed that fast ions are well-confined in MST [28], so ion energy can be ratcheted-up during successive reconnection events.

Fermi acceleration is a second candidate mechanism, one that naturally leads to a power law spectrum. The close proximity of tearing mode resonant surfaces in MST results in magnetic islands - small regions of private flux embedded in a larger magnetic topology. Particles can become trapped in these islands, and, as the islands contract, gain energy with each reflection. This mechanism has been applied to both the Earth's magnetosphere and solar flares [17].

The current measurements are unable to distinguish between these mechanisms, but a measurement of the parallel neutral energy spectrum may be able to. One would expect the parallel fast ion population to be much larger than the perpendicular fast ion population if they are generated by electric field acceleration, for example.

In summary, new measurements on MST have revealed previously unknown details about the majority and impurity ion distribution functions during magnetic reconnection. The impurity C^{+6} ion distribution function is found to be anisotropic with $T_{\perp} > T_{\parallel}$ near the reconnection event, suggesting a heating mechanism favoring the perpendicular degree of freedom. This anisotropy is observed to increase in size with increas-

ing plasma density, possibly due to varying impurity content in the plasma. The majority ion distribution function is found to be very nearly Maxwellian, but there exists a tail of fast ions which is generated at the reconnection event. It is well-described by a power-law and completely dominates neutron production. Both of these features may be used to evaluate models of ion energization from magnetic reconnection.

One author (R.M.) acknowledges valuable discussion regarding the CHERS data with Dr. Darren Craig and the careful reading and feedback provided by Dr. John Sarff during the preparation of the manuscript. This work is supported by the US DOE and NSF.

* richard.magee@mail.wvu.edu

† Currently at Laboratory for Laser Energetics, Rochester, NY, 14623, USA

- [1] B. B. Jones and R. Wilson, Nuclear Fusion Supplement **3**, 889 (1962).
- [2] R. B. Howell and H. J. Karr, The Physics of Fluids **19**, 2012 (1976).
- [3] R. B. Howell and Y. Nagayama, Phys. Fluids **28**, 743 (1985).
- [4] E. Scime *et al.*, Phys. Rev. Lett. **68**, 2165 (1992).
- [5] S. C. Hsu *et al.*, Physics of Plasmas **8**, 3859 (2001).
- [6] E. R. Priest *et al.*, Nature **393**, 545 (1998).
- [7] S. R. Cranmer, G. B. Field, and J. L. Kohl, The Astrophysical Journal **518**, 937 (1999).
- [8] R. N. Dexter *et al.*, Fusion Technology **19**, 131 (1991).
- [9] G. Fiksel, *et al.*, Phys. Rev. Lett. **103**, 145002 (2009).
- [10] N. Mattor, P. W. Terry, and S. C. Prager, Comments Plasma Phys. Controlled Fusion **15**, 65 (1992).
- [11] V. Tangri, P. W. Terry, and G. Fiksel, Physics of Plasmas **15**, 112501, (2008).
- [12] C. G. Gimblett, Europhys. Lett. **11**, 541 (1990).
- [13] V. A. Svidzinski, *et al.*, Physics of Plasmas **15**, 062511, (2008).
- [14] H. P. Furth and P. H. Rutherford, Phys. Rev. Lett. **28**, 545 (1972).
- [15] P. Helander, *et al.*, Phys. Rev. Lett. **89**, 235002, (2002).
- [16] M. R. Brown, *et al.*, Physics of Plasmas **9**, 2077, (2002).
- [17] J. F. Drake, *et al.*, Nature **443**, 553 (2006).
- [18] E. Scime, *et al.*, Phys. Fluids B **4**, 4062 (1992).
- [19] H. A. B. Bodin and A. A. Newton, Nuclear Fusion **20**, 1255 (1980).
- [20] T. D. Tharp, *et al.*, Physics of Plasmas **17**, 120701, (2010).
- [21] S. Gangadhara, *et al.*, Physics of Plasmas **15**, 056121, (2008).
- [22] D. Craig, *et al.*, Review of Scientific Instruments **72**, 1008 (2001).
- [23] D. J. Den Hartog, *et al.*, Review of Scientific Instruments **77**, 10F122, (2006).
- [24] R. M. Magee, *et al.*, Review of Scientific Instruments **81**, 10D716 (2010).
- [25] K. Sasaki, *et al.*, Plasma Phys. Control Fusion **39**, 333 (1997).
- [26] J. C. Reardon, *et al.*, Review of Scientific Instruments **72**, 598, (2001).
- [27] E. D. Mezonlin, *et al.*, Review of Scientific Instruments **78**, 053504, (2007).
- [28] G. Fiksel, *et al.*, Phys. Rev. Lett. **95**, 125001, (2005).